August 28, 1990

Warsaw University Preprint *IFD/6/1990*

New AMY and DELPHI multiplicity data and the lognormal distribution

R.Szwed, G.Wrochna and A.K.Wróblewski

Institute of Experimental Physics

Warsaw University

PL-00-681 Warsaw, ul. Hoża 69

Abstract

Multiplicity distributions for $e^+e^- \to$ *hadrons* recently reported by the AMY and DELPHI collaborations are compared to the data obtained at lower energies. It is proven that the new data obey the KNO–G scaling and the scaling function can be described by the lognormal distribution. The dispersions are linear functions of the mean as for the data measured at lower energies and the standardized moments (such as skewness and kurtosis) are independent of the energy. The energy dependence of the average multiplicity is described by $\langle n_{ch} \rangle = \beta\, s^{\alpha} - 1$.

1 Introduction

Recently new data on multiplicity distributions for the e^+e^-collisions by the two large collaborations AMY and DELPHI were published. Data obtained by the AMY collaboration [1] were obtained at the TRISTAN collider and cover the energy range $\sqrt{s} = 50 \div 61.4$ GeV. The DELPHI collaboration has published data taken at the LEP collider at $\sqrt{s} = 91$ GeV [2]. These new data are important because they extend considerably the energy range available for the study. In the following they are compared with the multiplicity data obtained at lower energies [3,4] and with earlier TRISTAN and LEP data [5].

We have found that the multiplicity distributions measured at lower energies (up to the $\sqrt{s} = 44$ GeV, TASSO data) obey the KNO-G scaling [6] and that they can be described by the lognormal distribution [7,8]. These facts can be explained by assuming that multiparticle production in e^+e^-interactions is a special kind of a branching process [8,9]. In the present paper we give the proof that the new data have similar properties as the earlier ones.

Section 2 contains the short description of a fitting procedure. The AMY and DELPHI data are analyzed in Sections 3 and 4. Section 5 is devoted to comparison of the various data. The dependence of the average multiplicity on the energy is discussed in Section 6.

2 Fitting procedure

The lognormal distribution is a continuous function whereas the multiplicity distribution is by definition a discrete function. Thus to calculate the probability P_n to produce n particles one should integrate the density $f(\tilde{n})$ (we use the tilde sign to stress the continuity of the variable [1]):

$$P_n = \int_n^{n+1} f(\tilde{n}) d\tilde{n} \ , \tag{2.1}$$

$$f(\tilde{n}) = \frac{N}{\sqrt{2\pi}\sigma} \cdot \frac{1}{\tilde{n} + c_f} \exp\left(- \frac{\left[\ln(\tilde{n} + c_f) - \mu_f\right]^2}{2\,\sigma^2} \right), \tag{2.2}$$

where c_f, μ_f, and σ are parameters and N is a normalization constant.

Obviously, formula (2.1) is written for n taking values $0, 1, 2, \ldots$. Thus before using this formula the experimentally measured charged multiplicity $n_{ch} = 0, 2, 4, \ldots$ should be converted into n ($n = n_{ch}/2$). The formulae (2.1) and (2.2) can be fitted directly to the data. However the parameters can vary with the collision energy. Thus we advocate to rewrite these formulae in a scale–invariant form

$$f(\tilde{n}) = \frac{1}{\langle \tilde{n} \rangle} \psi\left(\frac{\tilde{n}}{\langle \tilde{n} \rangle} \right) \tag{2.3}$$

and by substitution into (2.1)

$$\frac{\tilde{n}}{\langle \tilde{n} \rangle} = z \ , \qquad c_f = c\langle \tilde{n} \rangle \ , \qquad \mu_f = \mu + \ln\langle \tilde{n} \rangle \tag{2.4}$$

[1] The concept of the "continuous multiplicity" was introduced in this context in Ref. [6] and developed in [10]. See also Section 7 in Ref. [9].

we obtain

$$\psi(z) = \frac{N}{\sqrt{2\pi}\sigma} \cdot \frac{1}{z+c} \exp\left(-\frac{[\ln(z+c)-\mu]^2}{2\,\sigma^2}\right), \tag{2.5}$$

where $\langle\tilde{n}\rangle$ denotes the continuous average multiplicity defined as

$$\langle\tilde{n}\rangle = \int_0^\infty \tilde{n} f(\tilde{n}) d\tilde{n} = \int_0^\infty \tilde{n}\psi(z)dz \ . \tag{2.6}$$

The continuous mean multiplicity defined by (2.6) is different from the usual form $\langle n\rangle = \sum_{n=0}^{\infty} nP_n$, but for $\langle n\rangle \gtrsim 1$ it can be approximated by a simple formula (see Ref. [10])

$$\langle\tilde{n}\rangle \approx \langle n\rangle + 0.5 \ . \tag{2.7}$$

The scaling function $\psi(z)$ does not depend on the energy and all parameters of the lognormal distribution are constant.

It is worthwhile to mention that the dispersion of $\psi(z)$ is equal to

$$D = \sqrt{\langle z^2\rangle - \langle z\rangle^2} = \exp\left(\mu + \frac{\sigma^2}{2}\right) \cdot \sqrt{\exp(\sigma^2) - 1} \ . \tag{2.8}$$

In practice it is convenient to use the primitive function of $\psi(z)$ denoted by $\phi(z)$

$$\phi(z) = -\int_z^\infty \psi(z)dz = -\frac{N}{2}\,\mathrm{erfc}\left(\frac{\ln(z+c)-\mu}{\sqrt{2}\,\sigma}\right) \ . \tag{2.9}$$

The symbol "erfc" stands for the complementary error function [11]

$$\mathrm{erfc}(x) = \frac{2}{\sqrt{\pi}} \int_x^\infty e^{-t^2} dt \ . \tag{2.10}$$

Now the probability can be calculated as

$$P_n = \int_{n/\langle\tilde{n}\rangle}^{(n+1)/\langle\tilde{n}\rangle} \psi(z)dz = \phi\left(\frac{n+1}{\langle\tilde{n}\rangle}\right) - \phi\left(\frac{n}{\langle\tilde{n}\rangle}\right). \tag{2.11}$$

The scaling of the above form is called the "KNO–G scaling" [6,10] to be distinguished from the usual KNO scaling [12]

$$P_n = \frac{1}{\langle n\rangle}\,\psi_{KNO}\left(\frac{n}{\langle n\rangle}\right) \ . \tag{2.12}$$

Parameter N is given by the first normalization condition

$$\sum_0^\infty P_n = \int_0^\infty f(\tilde{n})d\tilde{n} = \int_0^\infty \psi(z)dz = -\phi(0) = 1 \ . \tag{2.13}$$

Hence[2]

[2]We assume that $c > 0$. If $c \leq 0$ then $N = 1$.

$$N = 2 \,/\, \mathrm{erfc}\left(\frac{\ln c - \mu}{\sqrt{2}\,\sigma}\right) . \tag{2.14}$$

Parameters μ, c and σ are constrained by the second normalization condition

$$\langle z \rangle = \int_0^\infty z\psi(z)dz = -\int_0^\infty \phi(z)dz = 1 . \tag{2.15}$$

Hence

$$\frac{\mathrm{erfc}\left(\nu - \sigma/\sqrt{2}\right)}{\mathrm{erfc}\,(\nu)} \cdot \exp\left(\mu + \frac{\sigma^2}{2}\right) - c = 1 , \quad \text{where} \quad \nu = \frac{\ln c - \mu}{\sqrt{2}\,\sigma} . \tag{2.16}$$

However, for not too large σ and c (which is the case in e^+e^- multiplicity distribution) one can use the approximations

$$N \approx 1 , \quad \exp\left(\mu + \frac{\sigma^2}{2}\right) - c \approx 1 . \tag{2.17}$$

Thus because of the normalization conditions (2.14) and (2.16) the lognormal function $\psi(z)$ has only two free parameters. In principle one can fit e.g. μ and σ and calculate N and c just from these conditions. However μ and σ are strongly correlated, thus the fitting procedure is unstable and obtained values of μ and σ are more or less accidental. Moreover, a correct error analysis is almost impossible.

A better solution is to take the weakly correlated shift c and dispersion D as free parameters to be fitted and then calculate μ and σ from (2.17) and (2.8)

$$\sigma = \sqrt{\ln\left[\left(\frac{D}{1+c}\right)^2 + 1\right]} , \quad \mu = \ln(c+1) - \frac{\sigma^2}{2} . \tag{2.18}$$

Then c, μ and σ can be substituted into (2.9) and P_n calculated from (2.11).

3 DELPHI data

In the new DELPHI collaboration paper [2] the fit of the lognormal distribution to the data is done according to the formulae (2.1) and (2.2), except that the charged multiplicity n_{ch} was not converted into $n = n_{ch}/2$ before fitting (see the sentence below the formula (2.2)). Therefore we add superscript "ch" to their parameters c_f and μ_f

$$c_f^{ch} = 7.5 \pm 2.3, \quad \mu_f^{ch} = 3.36 \pm 0.08 \text{ and } \sigma = 0.214 \pm 0.018 \text{ with } \chi^2/NDF = 4/18.$$

Using (2.4) (but with $2\langle\tilde{n}\rangle$ instead of $\langle\tilde{n}\rangle$) and (2.8) these DELPHI values can be approximately converted to

$$c = 0.33, \quad \mu = 0.254 \quad \text{and} \quad D = 0.285 .$$

Treating c and D as free parameters we have obtained

$$c = 0.27 \pm 0.12 \quad \text{and} \quad D = 0.284 \pm 0.007$$

with the similar χ^2 as obtained by DELPHI (see Table 1). The fitted lognormal distribution is presented in Fig. 1 as a continuous line in linear and logarithmic scale. In the same figure the dotted line represents a global fit to various experiments, which is discussed in Sec.5.

In our opinion the most sensitive test of the goodness of the fit is the ratio of measured to calculated distribution. The DELPHI data and the lognormal distribution are presented in this manner in Fig. 2. It is seen that there are no systematic deviations and the statistical fluctuations are within the range of errors.

Another convenient test for the lognormal distribution is the probit diagram because it converts the lognormal curve to the straight line. The definition of the probit diagram is presented e.g. in Ref. [13]. The explanation of how to apply it to the multiplicity distribution is given in Ref. [8,9]. The probit diagram for the DELPHI data is shown in Fig. 3.

4 AMY data

The AMY collaboration have measured multiplicity distribution at eight energies in the range $\sqrt{s} = 50 \div 61.4$ GeV [1]. In order to increase statistics the authors published also combined data, calling them: the 57 GeV data. However in our opinion the procedure of combining data is in this case unacceptable because careful checking of the tables presented by the AMY collaboration shows considerable energy dependence at the tails of the distributions. The only way to compare distributions at various energies is to use their scaling properties. However in doing this one should remember differences between the KNO–G and the usual KNO scaling. In case of the KNO–G the invariant reduced multiplicity should be defined as $z = n/\langle\tilde{n}\rangle$ [6,10]. However in the investigated energy range the approximation (2.7) can be used

$$z = \frac{n}{\langle\tilde{n}\rangle} \approx \frac{n}{\langle n\rangle + 0.5} \approx \frac{n_{ch}}{\langle n_{ch}\rangle + 1} \,. \tag{4.1}$$

To produce a plot for the KNO–G, which is equivalent to the standard KNO plot, we should approximate the integral in (2.11) by the value at the middle of the integration range

$$\begin{aligned} P_n &= \int\limits_{n/\langle\tilde{n}\rangle}^{(n+1)/\langle\tilde{n}\rangle} \psi(z)dz \approx \frac{1}{\langle\tilde{n}\rangle}\,\psi\left(\frac{n+0.5}{\langle\tilde{n}\rangle}\right) \approx \frac{1}{\langle n\rangle + 0.5}\,\psi\left(\frac{n+0.5}{\langle n\rangle + 0.5}\right) = \\ &= \frac{1}{\langle n_{ch}\rangle + 1}\,\psi\left(\frac{n_{ch}+1}{\langle n_{ch}\rangle + 1}\right) \,. \end{aligned} \tag{4.2}$$

Thus instead of usually plotted

$$\langle n_{ch}\rangle \cdot P_{n_{ch}} \quad \text{versus} \quad \frac{n_{ch}}{\langle n_{ch}\rangle} \tag{4.3}$$

for the KNO–G we should plot

$$(\langle n_{ch}\rangle + 1) \cdot P_{n_{ch}} \quad \text{versus} \quad \frac{n_{ch}+1}{\langle n_{ch}\rangle + 1} \,. \tag{4.4}$$

The AMY data at different energies are presented in this manner in Fig. 4.

We have fitted the lognormal distribution to each of the AMY distributions separately in the way described in Sec. 2. The results are given in Table 1. All the AMY data were also fitted simultaneously (see Table 1), and a very good χ^2 was obtained ($\chi^2/NDF = 0.35$).

The resulting curve is plotted in Fig. 4 as a dashed line. Taking into account the value of χ^2 and the graphical presentation in Fig. 4 one might conclude that the fit is very satisfactory. However, a more sensitive test presented in Fig. 5a shows that this fit is not good at all! The large systematic deviation of the fitted distribution from the data are seen.[3]

We have checked that this situation results from only a few highest multiplicity data points which have very large errors, comparable with the value of the probability itself. Thus the fit was repeated after removing the last three points from each distribution. This cut is equivalent to taking $z \lesssim 1.9$. The resulting curve is plotted in Fig. 4 as a continuous line and values of the parameters are given in Table 1. After the cut the ratio $P_n(exp.)/P_n(fit)$, which is presented in Fig. 5b, shows much smaller systematic deviations from unity.

We have also compared the global fit to the whole collection of data [3,4,5] (Sec.5) with the AMY data. This fit is shown in Fig. 4 as a dotted line.

Figure 6 presents the probit diagram for the AMY data which again proves the lognormal shape of the data.

5 Comparison of data at various energies

It was mentioned in Sec. 2 that if the data obey scaling then the parameters of the lognormal distribution should not vary with the energy. We have checked it explicitly. The lognormal distribution was fitted to each of data sets measured by LENA, JADE, HRS, TASSO, AMY and DELPHI collaborations [1,2,4]. The resulting values of c, D and χ^2 are given in Table 1. The dependence of c and D on the energy is plotted in Fig. 7.

It is obvious from Table 1 and Fig. 7 that the parameters indeed seem to be independent of the collision energy. However some systematic differences between experiments exceeding the plotted statistical errors are seen.

Parameter D is just the width of a distribution. Thus the value of D for the HRS data is considerably lower than for all other distributions, which confirms the well known fact that the distribution measured by the HRS experiment is narrower than others. Also the value of χ^2/NDF for HRS data is largest.

The set of fitted c parameters has more complicated structure. The JADE distributions are characterized by the lowest values of c. The AMY and DELPHI values of c lay in the middle. The highest values of c are characteristic for the LENA, HRS and TASSO data.

The differences described above mean that the studied distributions differ slightly in the lowest multiplicities to which the parameter c is sensitive. It seems to be understandable because usually low multiplicity events are not observed experimentally and published values for these topologies are taken from Monte Carlo programs. Thus the

[3]It is a good illustration of an obvious (but often forgotten) fact that sometimes the minimum of the χ^2 does not define the best approximation and that the value of the χ^2 can be misleading even if it is accompanied by a graphical presentation which is not sensitive enough to systematic deviations.

differences between the fitted values of c show the differences between the various Monte Carlo programs rather than between experimentally measured data.

Thus we may conclude that the absence of a systematic dependence of the fitted parameters on the energy proves again the scaling. Data measured at various energies can be described by a unique lognormal distribution.

To estimate the parameters of this unique distribution we have applied the fitting procedure described in Sec. 2 to all data sets at once. The results are given in Table 1 for the whole sample as well as for the individual distributions. The comparison of the global fit with the AMY and DELPHI data is presented in Figs. 1 and 4 where the dotted curve represents the global fit.

Another way to compare various data and to study the scaling properties is to check the behavior of certain statistical moments. The KNO–G scaling predicts that the dispersions

$$D_k = [\sum_{n_{ch}=2}^{\infty} (n_{ch} - \langle n_{ch} \rangle)^k P_{n_{ch}}]^{\frac{1}{k}} \tag{5.1}$$

are linear functions of the mean and the standardized moments

$$\varphi = \frac{\langle n_{ch} \rangle + 1}{D_2} \tag{5.2}$$

$$\gamma_1 = \left(\frac{D_3}{D_2}\right)^3 \quad \text{(skewness)} \tag{5.3}$$

$$\gamma_2 = \left(\frac{D_4}{D_2}\right)^4 \quad \text{(kurtosis)} \tag{5.4}$$

are constants.

Figs. 8 and 9, in which the above mentioned moments are plotted as functions of the average multiplicity, confirm above mentioned properties. The line in Fig. 8 is calculated using the global fit described above.

6 The average multiplicity

The bivariate branching process [8,9] – the same mechanism which implies the lognormal shape of the multiplicity distribution – predicts for the average multiplicity

$$\langle \tilde{n} \rangle = \tilde{\beta}\, s^{\alpha} \tag{6.1}$$

or (using approximation (2.7))

$$\langle n_{ch} \rangle = \beta\, s^{\alpha} - 1\ . \tag{6.2}$$

The fit to the data [3,4,5] presented in Ref. [8] gives $\alpha = 0.221$ and $\beta = 2.96$. The resulting curve is presented in Fig. 10. The new AMY [1] and DELPHI [2] data are also plotted in this figure. A good agreement of the new data with the line (6.2) is seen.

As a side remark we would like to mention that the unity in (6.2) is not a particular feature of our branching approach. In fact all published models which predict the power low for the average multiplicity obtain such behavior in the continuous limit. It means that they give the power low for the continuous mean multiplicity $\langle \tilde{n} \rangle$ (6.1) rather than for the discrete one $\langle n_{ch} \rangle = \beta\, s^{\alpha}$, which is usually suggested. Thus careful investigation shows that the unity as in (6.2) should appear in all models predicting the power low for the increase in the mean multiplicity with the energy.

7 Conclusions

It was checked that the AMY and DELPHI multiplicity data which doubled the available energy range for e^+e^-collisions have the same properties as observed for data obtained in experiments at lower energies. All available data can be described by the unique lognormal distribution using scaling variables.

The possible explanation of that fact was presented in Ref. [8,9]. The lognormal distribution appears as a result of a special kind of a branching process (bivariate branching) described in [8]. A characteristic feature of this branching process which makes it more realistic than others is that it is evaluated in the two variables: multiplicity and energy simultaneously.

A good agreement between prediction given in our earlier papers [7,8] and the new AMY and DELPHI multiplicity data may prove the value of proposed multiparticle production mechanism.

References

[1] *AMY* (50.0, 52.0, 55.0, 56.0, 57.0, 60.0, 60.8, 61.4 GeV) H.W.Zheng et al.: KEK preprint 90-005, University of Rochester preprint UR-1155, ER-13065-616 (June 1990), submitted to Phys. Rev. D

[2] *DELPHI* (91 GeV) DELPHI collaboration: CERN-EP Preprint, paper no.737 submitted to the 25th Int. Conf. on High Energy Physics, Singapore, August 1990

[3] *ADONE-MEA* (1.46–1.79 GeV) B.Esposito et al.: Lett. Nuovo Cim. 30 (1981) 65
ADONE $\gamma\gamma$ – 2 (1.43–2.87 GeV) C.Bacci et al.: Phys. Lett. 86B (1979) 234
MARK I (2.6–6.3 GeV) J.L.Siegrist et al.: Phys. Rev. D26, (1982) 969
CLEO (10.5 GeV) M.S.Alam et al.: Phys. Rev. Lett. 49 (1982) 357
PLUTO (9.4, 12.0, 13.0, 17.0, 22.0, 27.5, 30.6 GeV) Ch.Berger et al.: Phys. Lett. 95B (1980) 313

[4] *LENA* (7.4, 8.9, 9.3 GeV) B.Niczyporuk et al.: Z. Phys. C – Particles and Fields 9 (1981) 1
JADE (12, 30, 35 GeV) W.Bartel et al.: Z. Phys. C – Particles and Fields 20 (1983) 187
HRS (29 GeV) M.Derrick et al.: Phys. Rev. D34 (1986) 3304
TASSO (14.0, 22.0, 34.8, 43.6 GeV) W.Braunschweig et al.: Z. Phys. C – Particles and Fields 45 (1989) 1939

[5] *TOPAZ* (52.5, 55.5 GeV) Proc. of the XXIV Int.Conf.on HEP (Springer–Verlag,1988)
MARK II (91 GeV) Proc. of Madrid Conf. 1989 *ALEPH* (91 GeV) D.Decamp et al.: Phys. Lett. 234B (1990) 209

[6] A.I.Golokhvastov: Sov. J. Nucl. Phys. 27 (1978) 430; 30 (1979) 128

[7] R.Szwed and G.Wrochna: Z. Phys. C – Particles and Fields 47 (1990) 449

[8] R.Szwed, G.Wrochna and A.K.Wróblewski: Warsaw University Preprint IFD/1/1990, to be published in Modern Physics Letters (1990)

[9] G.Wrochna: Warsaw University Preprint IFD/5/1990, to be published in Proceedings of the XIII Warsaw Symposium on Elementary Particle Physics, Kazimierz, Poland, May 1990

[10] R.Szwed and G.Wrochna: Z. Phys. C – Particles and Fields 29 (1985) 255

[11] W.H.Press, B.P.Flannery, S.A.Teukolsky and W.T.Vetterling: "Numerical Recipes", Cambridge University Press 1986, p. 164

[12] Z.Koba, H.B.Nielsen and P.Olesen: Nucl. Phys. B40 (1972) 317

[13] N.Arley and K.R.Buch: Introduction to the Theory of Probability and Statistics, New York 1950, Chapter 10, (John Wiley and Sons)

Figure captions

Fig. 1
The multiplicity distribution measured by the DELPHI collaboration [2] at $\sqrt{s} = 91$ GeV. Continuous line represents the fit to the DELPHI data, dotted line – the global fit to the whole data set described in the text and Table 1.

Fig. 2
The ratio of $P_n(exp.)/P_n(lognormal)$ plotted as a function of the reduced multiplicity $z = n/\langle\tilde{n}\rangle$ for the DELPHI data [2].

Fig. 3
Probit diagram for the DELPHI data [2].

Fig. 4
The multiplicity distributions measured by the AMY collaboration [1] plotted in approximately scale-invariant form (see text). Continuous line represents the fit to the AMY data without the last three points of each distribution, dashed line – fit to the AMY data with no cuts, dotted line – global fit to the data set described in the text and Table 1.

Fig. 5
The ratio of $P_n(exp.)/P_n(lognormal)$ plotted as a function of the reduced multiplicity $z = n/\langle\tilde{n}\rangle$ for the AMY data [1]. **(a)**: fit with no cuts, **(b)**: fit without the last three points from each distribution ($z \lesssim 1.9$).

Fig. 6
Probit diagram for the AMY data [1].

Fig. 7
Parameters of the lognormal distribution fits plotted as a function of the collision energy.

Fig. 8
The dispersions D_2, D_3 and D_4 plotted as a function of mean multiplicity for the e^+e^- data [1,2,4]. The solid line is calculated with the lognormal distribution globally fitted to the data set described in the text.

Fig. 9
The standardized moments φ, γ_1 and γ_2 plotted against the mean multiplicity for the e^+e^- data [1,2,4].

Fig. 10
The average multiplicity $\langle n_{ch}\rangle$ plotted as a function of centre of mass energy $\sqrt{s}$ for the multiplicity data measured by the indicated collaboration teams [1,2,3,4,5]. The solid line corresponds to the formula (6.2): $\langle n_{ch}\rangle = 2.96 \cdot s^{0.221} - 1$.

Table 1

Results of fits of the lognormal distribution to the e^+e^- multiplicity distributions.

Parameters obtained for each experimental data set are indicated in the left part of the table. At the bottom the parameters obtained for the whole collection of data (global fit) are given. In the right part of the table the goodness of the description of the individual data by the globally fitted lognormal distribution is presented.

Errors correspond to change of χ^2 of 1.

experiment	$\sqrt{s}$	fit to the specified data set						"global fit"		
		c	D	NDF	χ^2	χ^2/NDF	NDF	χ^2	χ^2/NDF
LENA	7.4	1.54 ± 4.00	0.298 ± 0.020	3	2.11	0.70	5	3.92	0.78
	8.9	0.64 ± 1.98	0.289 ± 0.045	3	10.95	3.65	5	11.35	2.27
	9.3	1.07 ± 2.37	0.300 ± 0.037	4	0.44	0.11	6	2.01	0.33
JADE	12.0	0.11 ± 0.54	0.316 ± 0.044	8	4.03	0.50	10	8.01	0.80
	30.0	0.00 ± 0.23	0.284 ± 0.023	11	3.92	0.36	13	6.57	0.51
	35.0	0.08 ± 0.46	0.293 ± 0.026	11	1.60	0.15	13	3.10	0.24
HRS	29.0	1.17 ± 0.32	0.262 ± 0.004	12	5.15	0.43	14	47.52	3.39
TASSO	14.0	0.66 ± 0.22	0.289 ± 0.006	11	8.82	0.80	13	19.81	1.52
	22.0	0.76 ± 0.23	0.284 ± 0.005	12	1.94	0.16	14	8.12	0.58
	34.8	0.73 ± 0.11	0.281 ± 0.003	16	9.21	0.58	18	21.24	1.18
	43.6	1.19 ± 0.27	0.282 ± 0.004	17	9.35	0.55	19	29.90	1.57
	all	0.81 ± 0.06	0.282 ± 0.002	62	41.47	0.67	64	79.07	1.24
AMY	50.0	0.50 ± 0.40	0.269 ± 0.018	14	1.95	0.14	16	3.98	0.25
$z \lesssim 1.9$	52.0	0.43 ± 0.28	0.279 ± 0.014	14	3.17	0.23	16	3.71	0.23
	55.0	0.48 ± 0.26	0.274 ± 0.014	14	1.13	0.08	16	2.50	0.16
	56.0	0.34 ± 0.22	0.290 ± 0.015	14	0.75	0.05	16	2.47	0.15
	57.0	0.39 ± 0.21	0.285 ± 0.017	14	1.52	0.11	16	2.82	0.18
	60.0	0.41 ± 0.30	0.288 ± 0.017	15	2.07	0.14	17	2.98	0.18
	60.8	0.29 ± 0.19	0.285 ± 0.016	15	0.94	0.06	17	6.41	0.38
	61.4	0.24 ± 0.19	0.288 ± 0.015	15	1.81	0.12	17	9.38	0.55
	all	0.35 ± 0.06	0.282 ± 0.004	129	19.05	0.15	131	34.25	0.26
no cuts	*all*	0.61 ± 0.06	0.268 ± 0.003	153	53.31	0.35	–	–	–
DELPHI	91.0	0.27 ± 0.12	0.284 ± 0.007	19	4.39	0.23	21	12.74	0.61
all		0.56 ± 0.03	0.277 ± 0.001	–	–	–	282	208.55	0.74

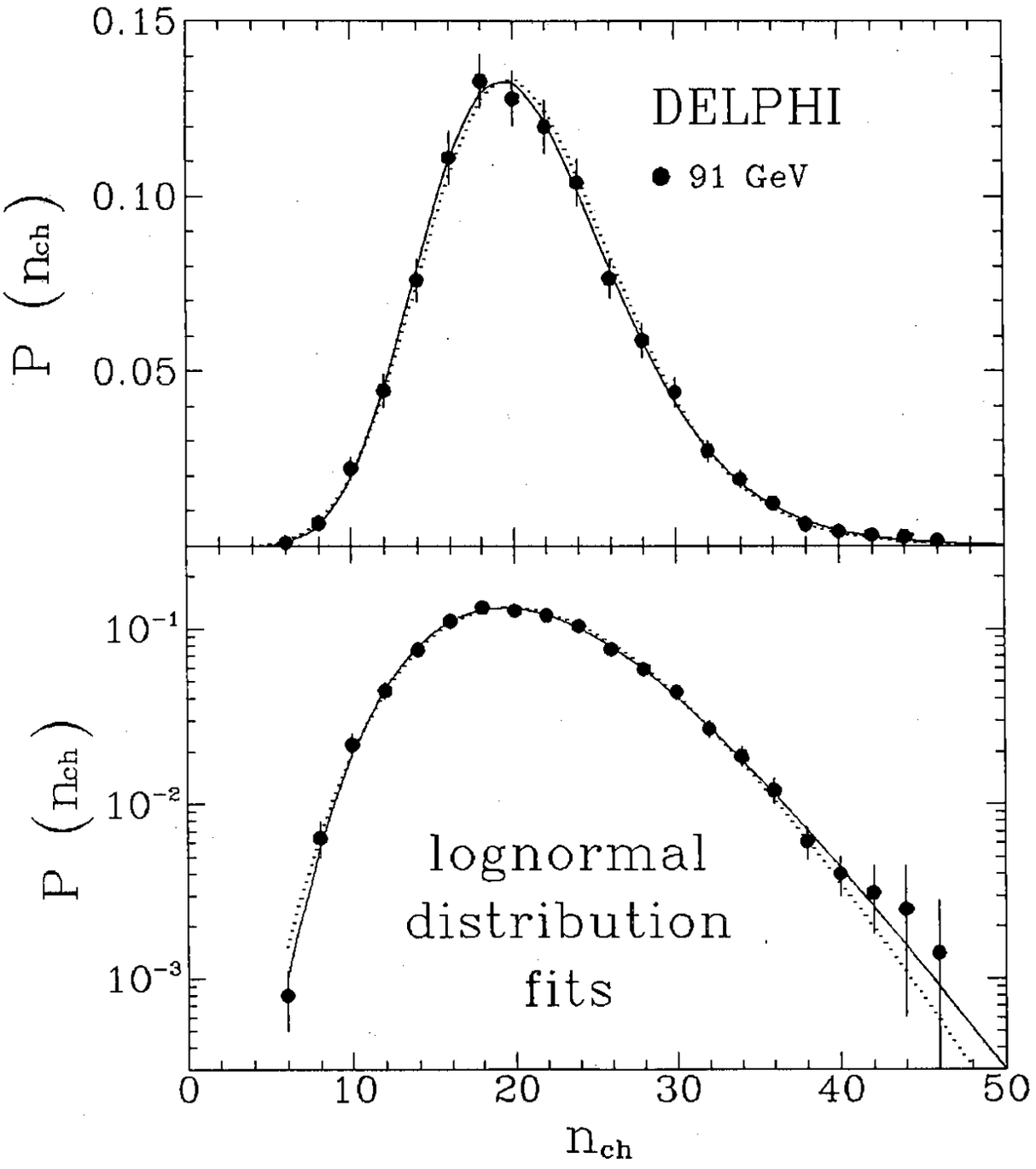
DELPHI
91 GeV
P (nch)
0.15
0.10
0.05
lognormal
distribution
fits
10⁻¹
10⁻²
10⁻³
0
10
20
30
40
50
nch

Fig.1

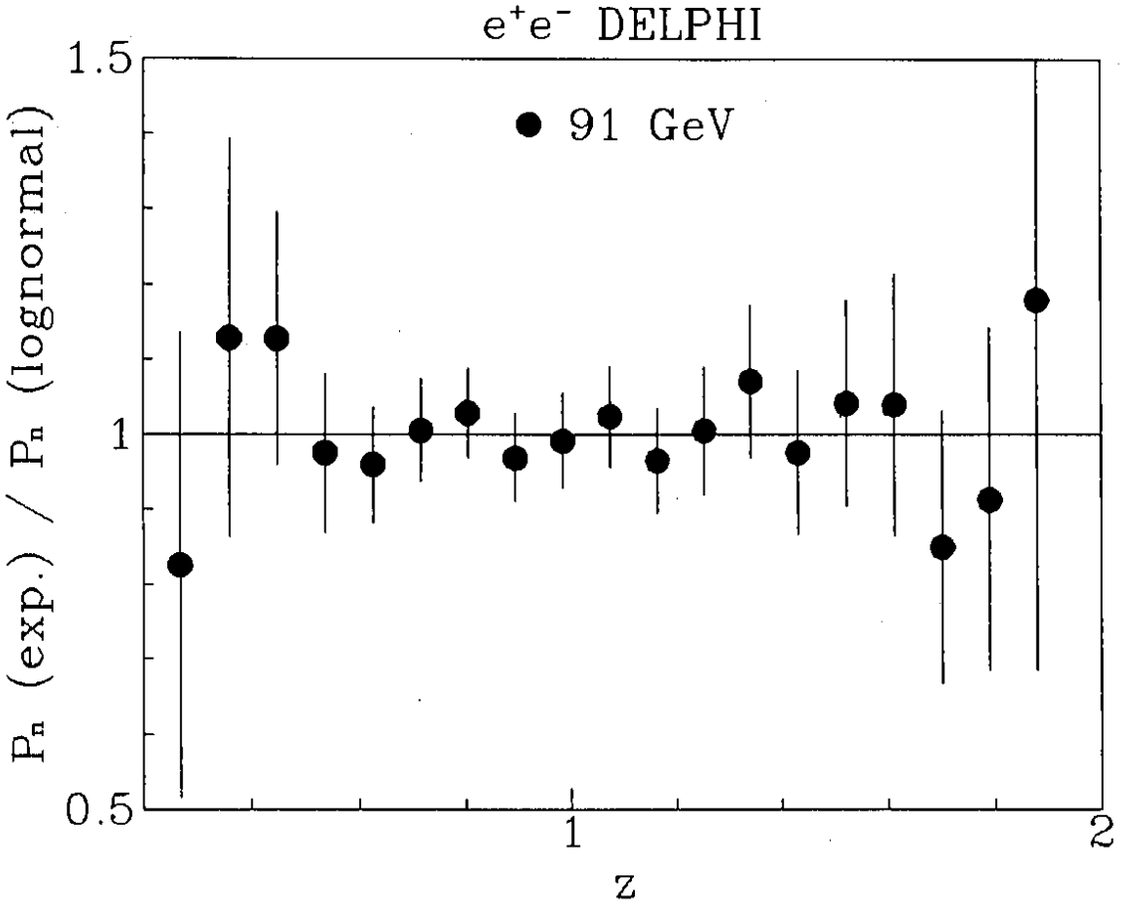

Fig.2

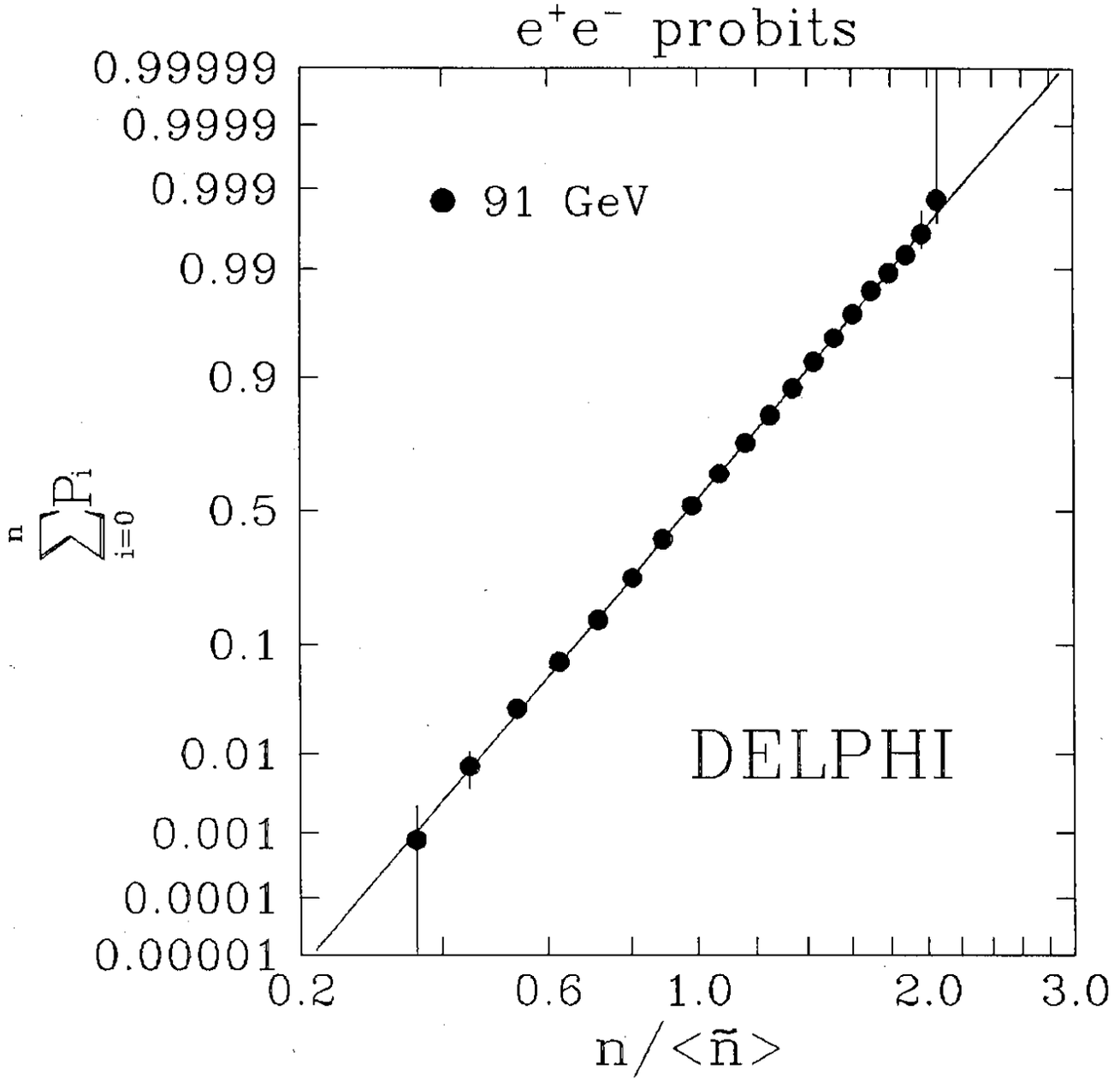
e+e− probits
0.99999
0.9999
0.999
0.99
0.9
0.5
0.1
0.01
0.001
0.0001
0.00001
n Σ Pi i=0
91 GeV
DELPHI
0.2
0.6
1.0
2.0
3.0
n/<ñ>

Fig.3

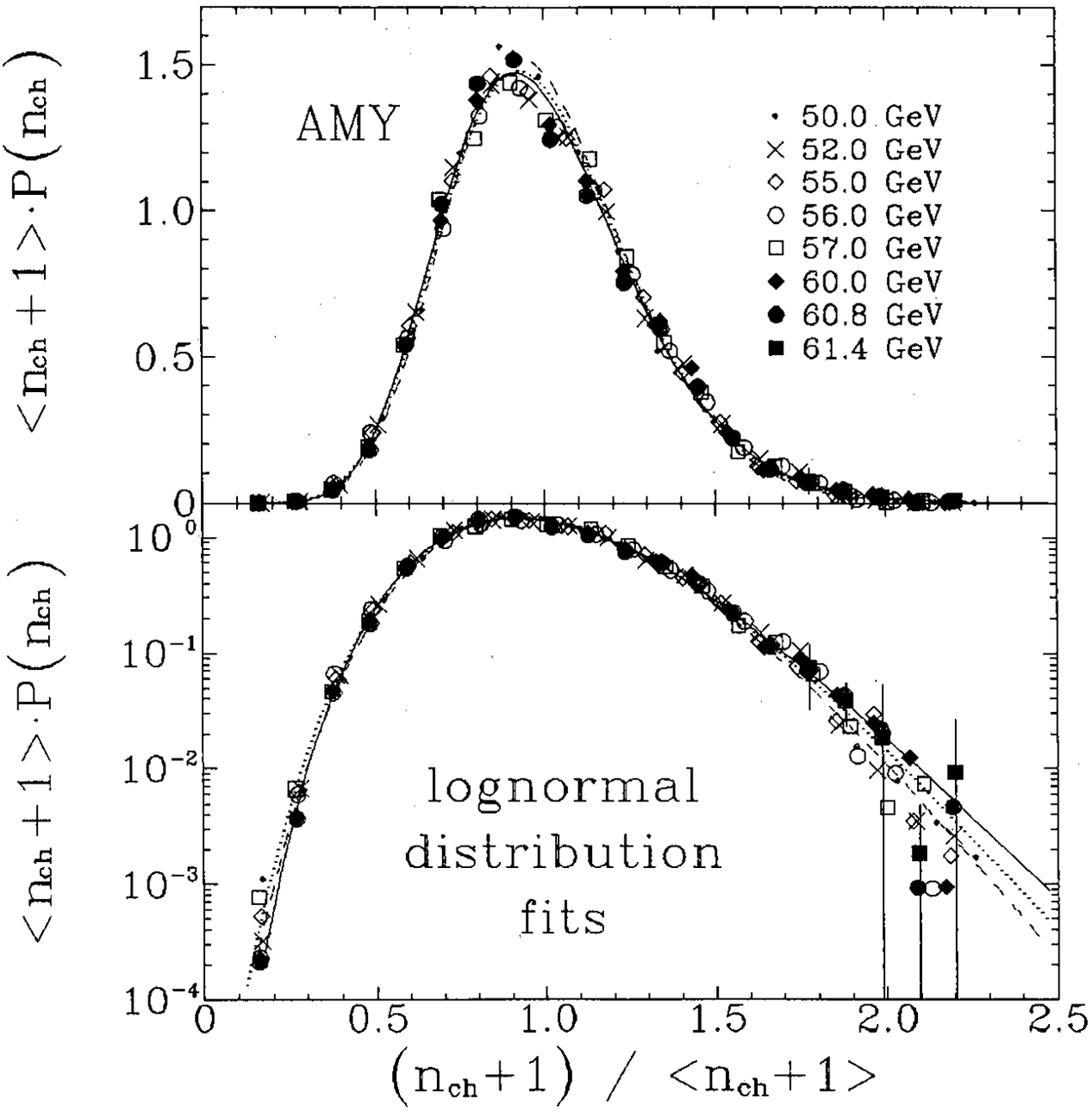
AMY
50.0 GeV
52.0 GeV
55.0 GeV
56.0 GeV
57.0 GeV
60.0 GeV
60.8 GeV
61.4 GeV
lognormal
distribution
fits
$\langle n_{ch}+1\rangle \cdot P(n_{ch})$
$(n_{ch}+1) \;/\; \langle n_{ch}+1\rangle$

Fig.4

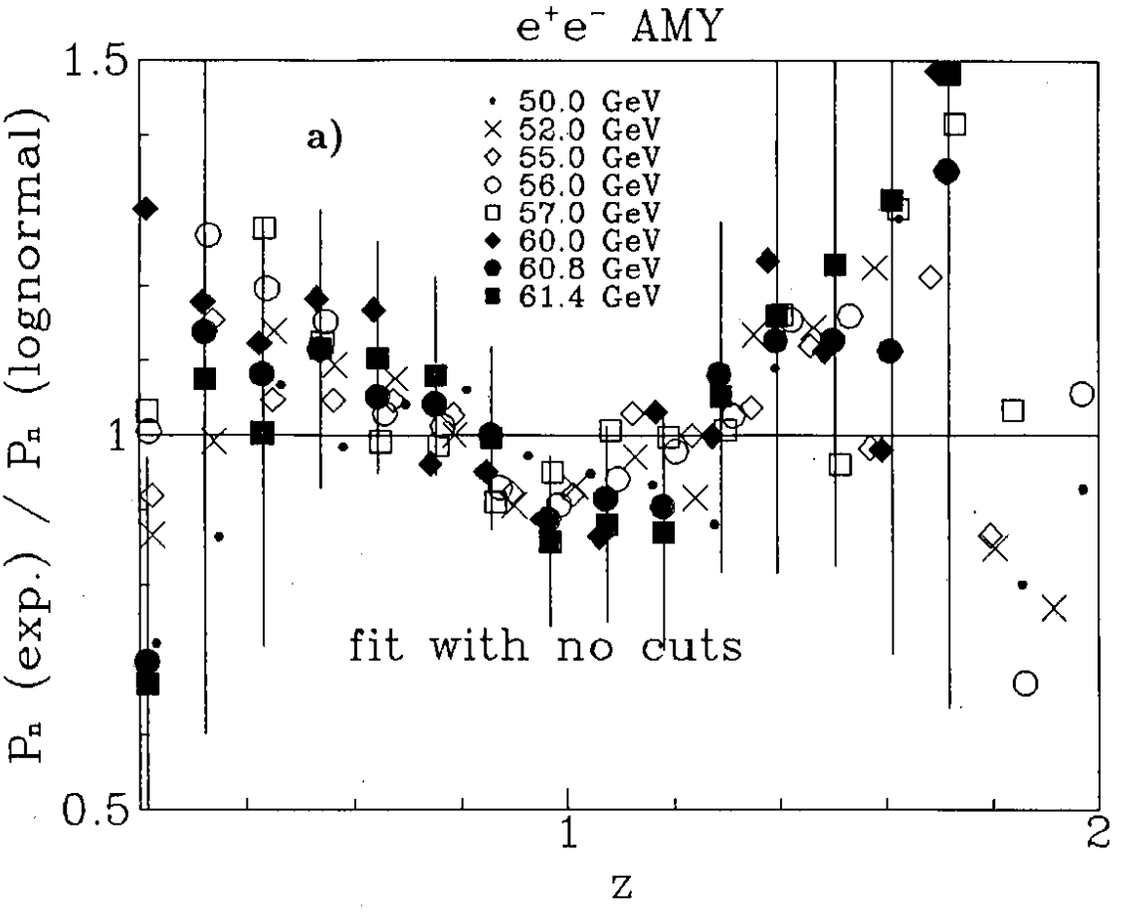
e+e- AMY
a)
50.0 GeV
52.0 GeV
55.0 GeV
56.0 GeV
57.0 GeV
60.0 GeV
60.8 GeV
61.4 GeV
fit with no cuts
Pn (exp.) / Pn (lognormal)
z
1.5
1
0.5
1
2

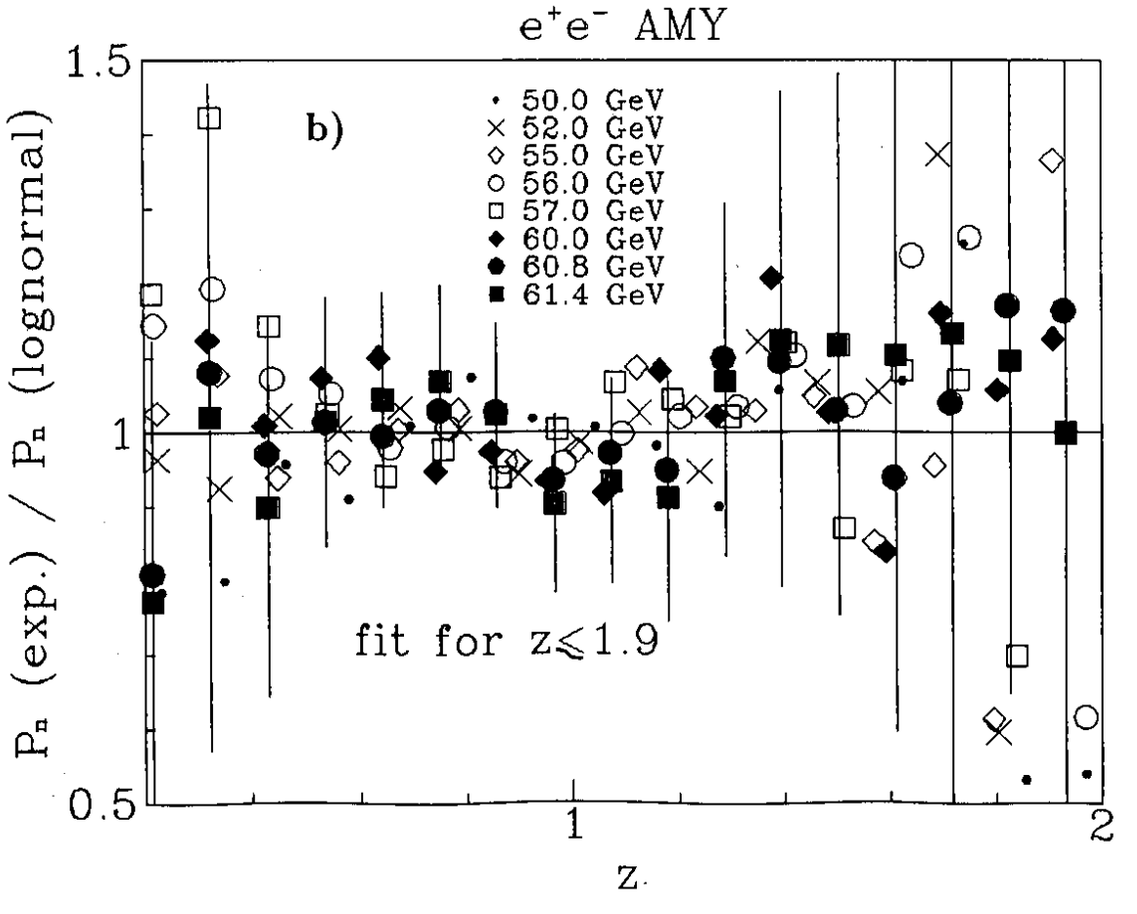
e+e- AMY
b)
50.0 GeV
52.0 GeV
55.0 GeV
56.0 GeV
57.0 GeV
60.0 GeV
60.8 GeV
61.4 GeV
fit for z≲1.9
Pn (exp.) / Pn (lognormal)
z
1.5
1
0.5
1
2

Fig.5

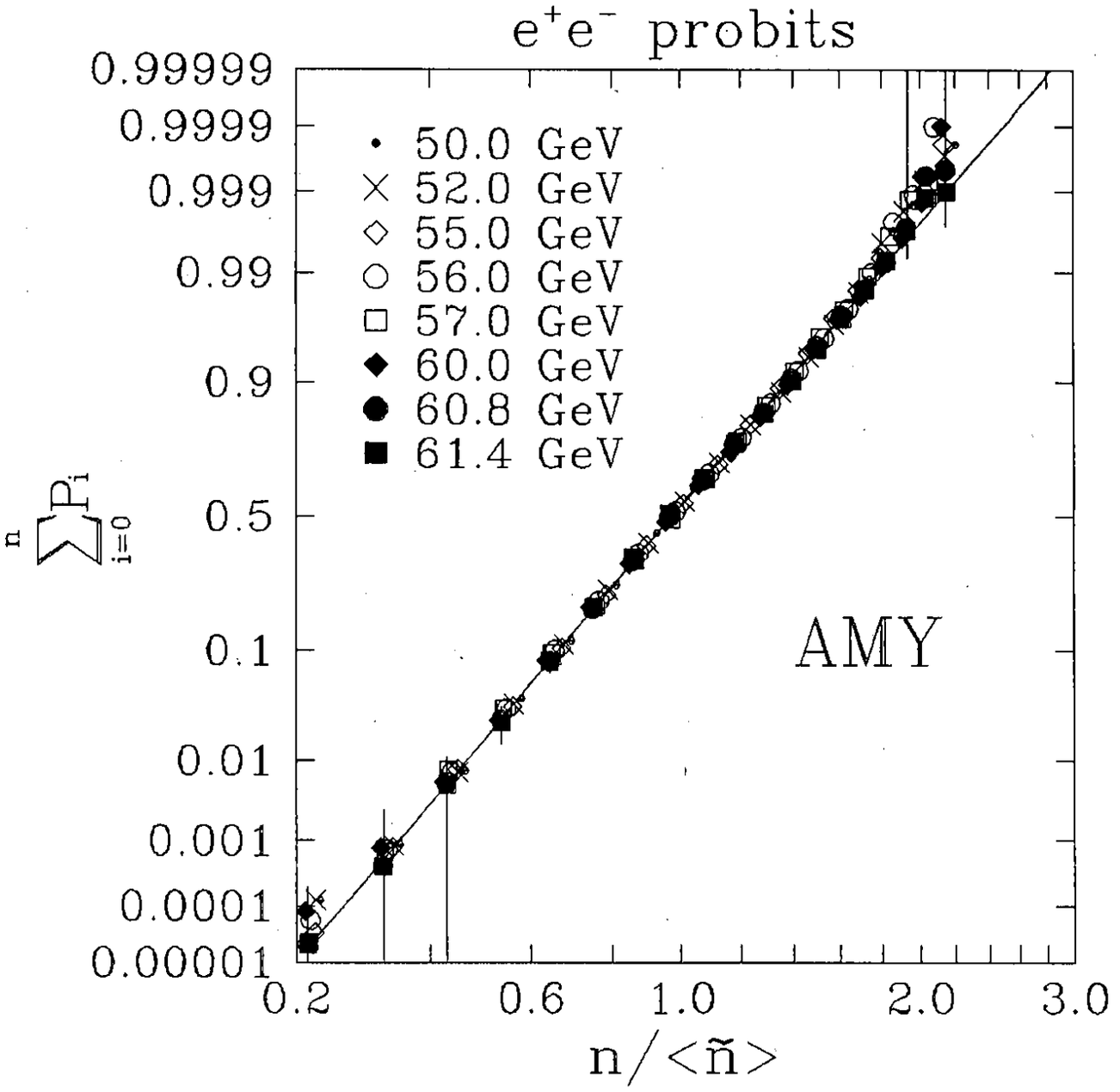
e+e- probits
0.99999
0.9999
0.999
0.99
0.9
0.5
0.1
0.01
0.001
0.0001
0.00001
50.0 GeV
52.0 GeV
55.0 GeV
56.0 GeV
57.0 GeV
60.0 GeV
60.8 GeV
61.4 GeV
AMY
0.2
0.6
1.0
2.0
3.0
n/<ñ>
n Σ Pi
i=0

Fig.6

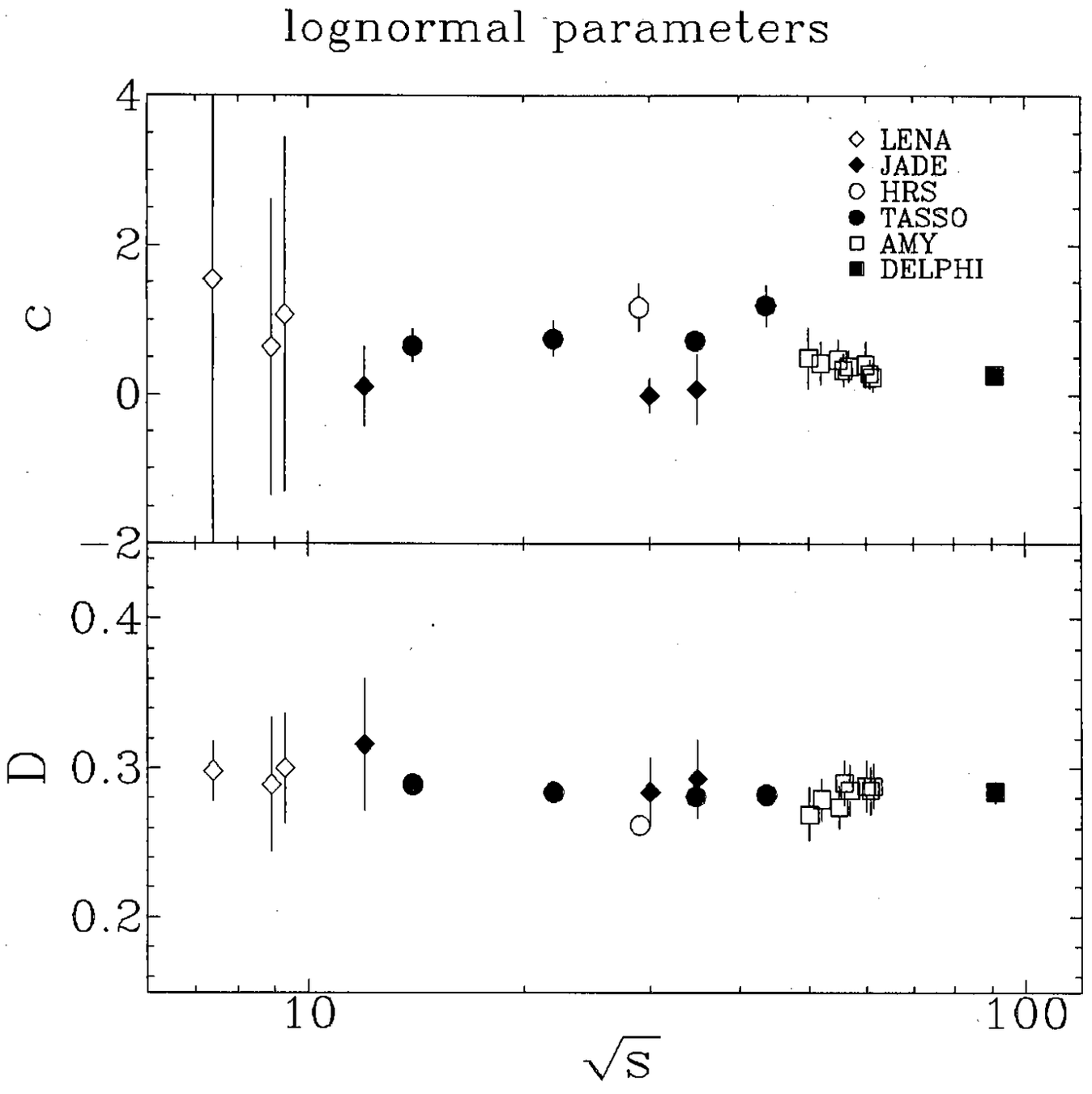
lognormal parameters
LENA
JADE
HRS
TASSO
AMY
DELPHI
c
D
$\sqrt{s}$
4
2
0
−2
0.4
0.3
0.2
10
100

Fig.7

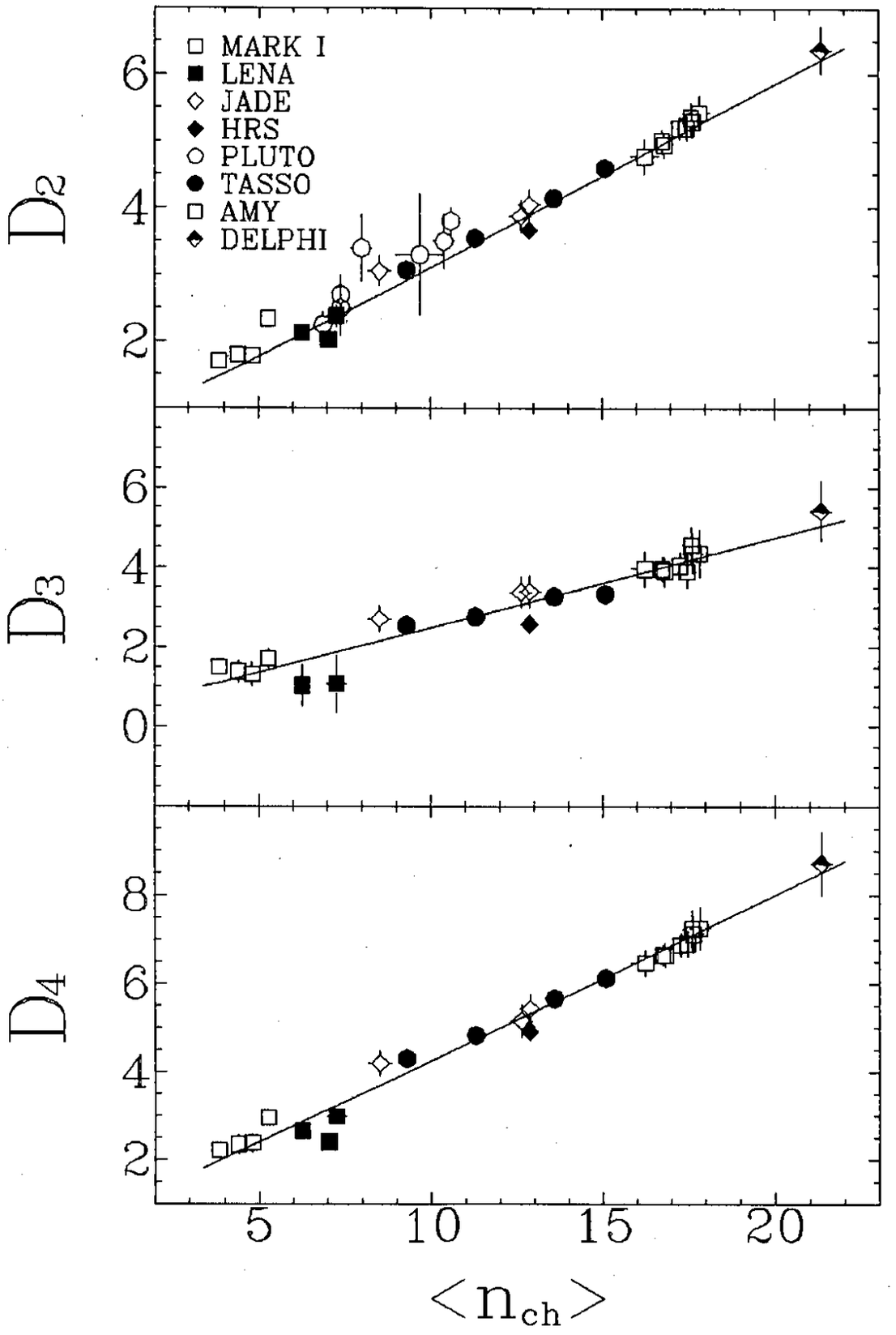
MARK I
LENA
JADE
HRS
PLUTO
TASSO
AMY
DELPHI
D2
D3
D4
<nch>
5
10
15
20

Fig.8

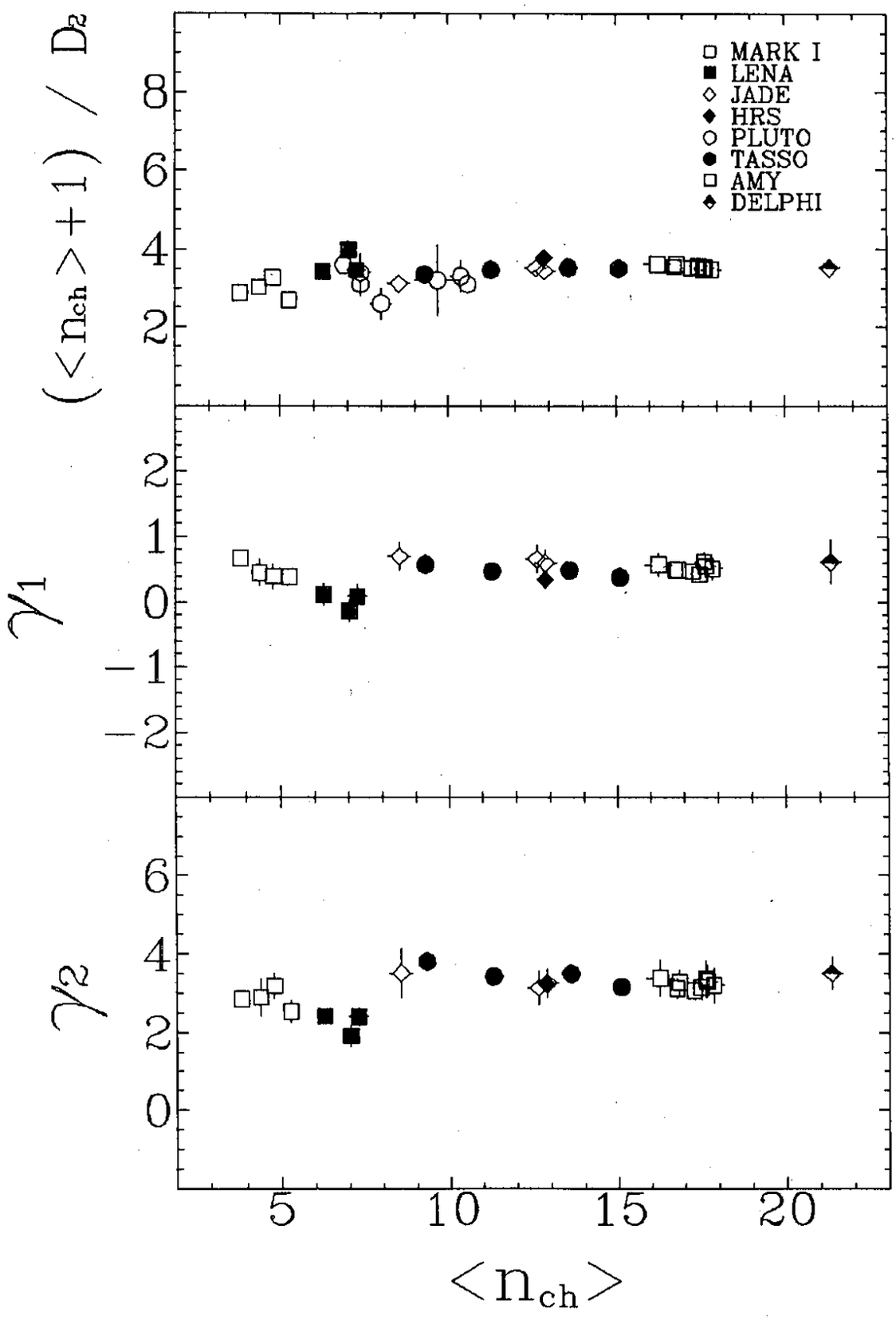
$(<n_{ch}>+1)\ /\ D_2$
MARK I
LENA
JADE
HRS
PLUTO
TASSO
AMY
DELPHI
γ_1
γ_2
$<n_{ch}>$

Fig.9

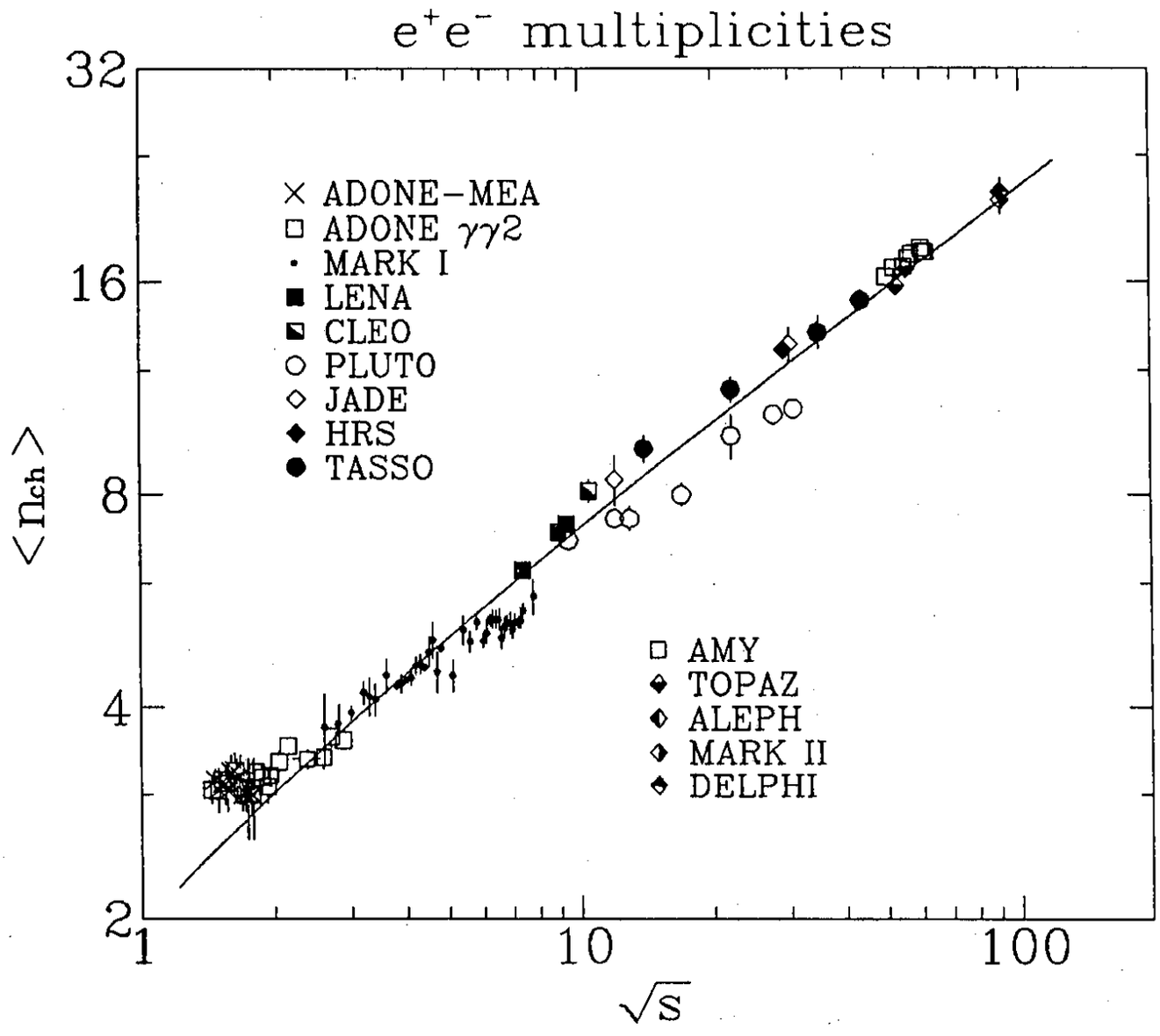
e+e- multiplicities
32
16
8
4
2
1
10
100
√s
<nch>
× ADONE-MEA
□ ADONE γγ2
· MARK I
■ LENA
◪ CLEO
○ PLUTO
◇ JADE
◆ HRS
● TASSO
□ AMY
◆ TOPAZ
◆ ALEPH
◆ MARK II
◆ DELPHI

Fig.10